



ADSORPTION OF METHYLENE BLUE FROM AQUEOUS SOLUTIONS BY ACTIVATED CARBON PREPARED FROM BANANA TRUNK USING ZINC CHLORIDE ACTIVATION

(Penjerapan Metilena Biru daripada Larutan Aqueus oleh Karbon Teraktif yang Disediakan dari Batang Pisang secara Pengaktifan Zink Klorida)

Zaidi Ab Ghani^{1*}, Muhammad Taufiq Hafizuddin R. Azemi¹, Mohd Hafiz Yaacob¹, Noor Hafizah Uyup¹,
Lee Sin Ang¹, Nor Azliza Akbar²

¹Faculty of Applied Science,

Universiti Teknologi MARA Cawangan Perlis, 02600 Arau Perlis, Malaysia.

²School of Civil Engineering, College of Engineering,

Universiti Teknologi MARA Cawangan Pulau Pinang, 13500 Permatang Pauh, Pulau Pinang, Malaysia

*Corresponding author: zaidi433@uitm.edu.my

Received: 10 September 2021; Accepted: 18 December 2021; Published: 28 April 2022

Abstract

In this study, the banana trunk-derived activated carbon (BTAC) used was prepared via zinc chloride (ZnCl_2) activation. BTAC is used as an adsorbent to remove methylene blue (MB) from the aqueous solutions. The BET surface area, total pore volume and pore diameters of the BTAC were $1329.5 \text{ m}^2/\text{g}$, $1.16 \text{ cm}^3/\text{g}$ and 3.8 nm , respectively. The effect of adsorbent dosage, initial concentration, contact time and solution pH were studied in batch experiments. The experimental data were analyzed by Langmuir, Freundlich, Temkin, and Dubinin-Radushkevich (D-R) adsorption isotherms model. Data analysis study via RMSE and χ^2 analyses suggested that Temkin isotherm model was the best fitted with the adsorption of MB on BTAC. The maximum monolayer adsorption of MB onto BTAC was calculated to be 217 mg/g . Kinetic parameters were evaluated based on pseudo-first-order (PFO), pseudo-second-order (PSO) and Weber–Morris intraparticle diffusion (IPD) kinetic models. The regression results showed that a PSO model is more accurately representing the adsorption kinetics. While the plot of q_t versus $t^{1/2}$ for the IPD model represented multi-linearity and proved that the adsorption processes occurred more than one step. Thermodynamics parameters were determined between temperatures of 25 to 40°C . The ΔG° and ΔH° values were negative and the overall adsorption process was determined as spontaneous and exothermic. While the positive value of ΔS° proposed good affinity of the MB molecules toward the BTAC. The results from this study suggested that BTAC could be a viable adsorbent in managing higher concentrations of dyes from water and wastewater.

Keywords: adsorption, activated carbon, methylene blue, isotherm, kinetic

Abstrak

Dalam kajian ini, karbon teraktif daripada batang pisang (BTAC) yang digunakan telah disediakan melalui pengaktifan zink klorida (ZnCl_2). BTAC telah digunakan sebagai penjerap untuk menyingkirkan metilena biru (MB) daripada larutan akueus. Keluasan permukaan BET, jumlah isipadu dan diameter liang pori bagi BTAC masing-masing adalah $1329.5 \text{ m}^2/\text{g}$, $1.16 \text{ cm}^3/\text{g}$

dan 3.8 nm. Kesan dos penyerap, kepekatan permulaan, masa kontak dan pH larutan dilakukan secara eksperimen kelompok. Data eksperimen telah dianalisa menggunakan model Langmuir, Freundlich, Temkin dan Dubinin–Radushkevich. Analisa data kajian melalui RMSE dan χ^2 mencadangkan bahawa model isoterma Temkin adalah yang paling sesuai dengan penyerapan MB pada BTAC. Penyerapan lapisan-mono maksima MB kepada BTAC dikira sebagai 217 mg/g. Parameter kinetik telah dinilai berdasarkan model kinetik pseudo-pertama (PFO), pseudo-kedua (PSO) dan resapan intrazarah (IPD) Weber–Morris. Hasil regresi menunjukkan bahawa model PSO lebih tepat mewakili kinetik penyerapan. Sementara plot q_t melawan $t^{1/2}$ untuk model IPD menunjukkan garisan linear yang pelbagai dan membuktikan bahawa proses penyerapan berlaku lebih daripada satu langkah. Parameter termodinamik telah ditentukan di antara suhu 25 hingga 40 °C. Nilai ΔG° dan ΔH° adalah negatif, maka keseluruhan proses penyerapan telah ditentukan sebagai spontan dan eksotermik. Sementara itu, nilai positif bagi ΔS° mencadangkan bahawa pertalian yang baik diantara molekul MB terhadap BTAC. Keputusan dari kajian ini mencadangkan bahawa BTAC mampu menjadi penyerap yang berkesan dalam menguruskan kepekatan pewarna yang lebih tinggi dari air dan air sisa.

Kata kunci: penyerapan, karbon teraktif, metilena biru, isoterma, kinetik

Introduction

Wastewater effluent that contains dyes is a typical and one of the major causes of environmental pollution. The presence of dyes in the industries effluent poses the most prominent problem since they are toxic and the recalcitrant nature of dyes [1]. Typical biological wastewater treatment plants cannot eliminate toxic pollutants such as dyes since they were purposely designed for organic and nutrient removal. Methylene blue (MB) is an example of dye that is commonly used in industry. MB is a heterocyclic aromatic chemical compound. Thus, MB is highly toxic, carcinogenic and its degradation process is difficult [2]. Therefore, MB containing effluent must be treated appropriately before discharge. Previously, various advanced oxidation methods have been introduced to treat dyes polluted water, such as ozonation [3], photocatalyst [4] and electrochemical treatment [5]. However, oxidation or degradation of dyes might contribute to the secondary pollutants. The other methods that have been employed include reverse osmosis [6], coagulation-flocculation [7], membrane filtration [8], ion exchange [9] and adsorption [10]. Among these methods, adsorption is a well-known and applicable method of removing dyes contaminant water. In addition, the adsorption process has emerged as a cost-effective, efficient, and environmentally friendly method of dye removal [11].

Recently, there are a variety of absorbents have been introduced to treat dyes such as bio-composite [12], nanoparticles [13], graphene oxide [14], forest wastes

[15], polystyrene foam [16] agriculture waste [17]. Based on the current scenario, activated carbon (AC) is the best adsorbent to treat textile effluent. Previously, the preparation of AC by using low-cost precursor from agriculture waste such as dates stone [18], ashitaba waste [19], banana peel [20], almond and walnut shells [21] have been employed extensively as a new precursor in the production of AC. Most of the mentioned researchers claimed that abundance and continuous availability of the agriculture biomass are the key motivation of their precursor selection. In addition, the treatment and reuse of agriculture waste should be implemented efficiently to obtain its valorization and achieve sustainable waste management [22].

In Malaysia, biomass derived from agriculture such as banana plantation is gaining increasing attention. Banana widely planted in tropical country such as Malaysia, thus it is not surprising that it is the major biomass source. Instead of burning and disposing naturally as an organic fertilizer, a better way would be converting them into AC. Thus, this study used banana trunk as a precursor to prepare AC. During preparation of AC via chemical activation, the lignocellulosic precursor is treated primarily with a chemical agent, such as H_3PO_4 , H_2SO_4 , HNO_3 , $NaOH$, KOH , or $ZnCl_2$. According to Lewoyehu [23], during the activation with $ZnCl_2$ the cellulosic material will be degraded, results in charring and aromatization of the carbon skeleton and creation of the pore structure. Hence,

produced AC with high surface area and good adsorption capacity.

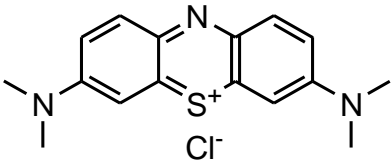
However, in order to treat water-containing dye via adsorption requires a deeper understanding especially on the effectiveness of the adsorbent towards the adsorbate. Therefore, the objective of the present work is to introduce BTAC as an adsorbent and to examine its effectiveness in removing MB from aqueous solutions. The effect of adsorbent dosage, initial concentration, contact time and solution pH were studied in batch experiments. The experimental were analyzed by Langmuir, Freundlich, Temkin, and Dubinin-Radushkevich (D-R) adsorption isotherms model. Kinetic parameters, rate constants, equilibrium adsorption capacities, and related correlation coefficients were evaluated based on pseudo-first-order (PFO), pseudo-second-order (PSO) and Weber–Morris intraparticle diffusion (IPD) kinetic models. Thermodynamics parameters such as ΔG° , ΔH° , and ΔS° have also were evaluated.

Materials and Methods

Materials

In this study, the adsorbent used was BTAC with particle size <215 μm , which was obtained from our previous study [24]. The BTAC was prepared from the banana trunk and activated with ZnCl_2 at a temperature of 640 $^\circ\text{C}$. All the chemicals used in this study were of analytical reagent grade unless otherwise stated. The adsorbate used is a cationic dye, namely methylene blue (Sigma Aldrich, Germany). The physicochemical information of BTAC and MB were shown in Table 1. MB adsorption data was used to obtain adsorption isotherms, kinetic and thermodynamic study. Stock solution of MB (1000 mg/L = 1000 ppm) was prepared by dissolving 1 g of MB into 1 L distilled water. The stock solution was further diluted with distilled water to obtain the desired concentrations of MB in the range of 75 to 125 mg/L .

Table 1. Physicochemical information of BTAC and MB[20]

Banana trunk derived activated carbon (BTAC)			
Textural properties		Ultimate analysis (wt.% dry basis)	
BET surface area (m^2/g)	1329.5	Carbon (wt%)	84.1
Mesopore surface area (m^2/g)	1152.6	Hydrogen (wt%)	2.1
Micropore surface area (m^2/g)	176.9	Nitrogen (wt%)	3.7
Total pore volume (cm^3/g)	1.16	Sulfur (wt%)	0.2
Pore diameter (nm)	3.83	Oxygen (wt%)	9.9
Physicochemical properties		Proximate analysis (wt.% dry basis)	
Bulk density (g/cm^3)	0.6	Volatile matter (wt%)	25.1
Iodine number (mg/g)	819.03	Fixed carbon (wt%)	74.7
pH_{pzc}	3.7	Ash (wt%)	0.2
Methylene blue (MB)			
 <p>Structure formula of MB</p>	Commercial name	Methylene blue	
	Chemical name	Methylthioninium chloride	
	Empirical formula	$\text{C}_{16}\text{H}_{18}\text{ClN}_3\text{S}$	
	Molar mass	319.85 g/mol	
	CAS number	61-73-4	
	λ_{max}	664 nm	

Batch adsorption study

The batch adsorption procedure was utilized to investigate the uptake of MB from aqueous solution onto BTAC. For the effect of adsorbent dosage, various dosage of BTAC ranging from 0.01 to 0.13 g was added into 250 mL Erlenmeyer flasks containing 100 mL of 150 mg/L MB concentration. The influence of initial concentration was explored using seven different concentrations from 50 to 150 mg/L MB solution. While the effect of contact time was determined from initial until equilibrium contact time is reached (5 to 360 min). The solution pH was varied from 5.0 to 8.0 with constant another adsorption parameter. The samples were then shaken at isothermal temperature (25 ± 2 °C) at 125 rpm in an incubator shaker. Each experiment was conducted with two replications. Then, the samples were taken out and filtered through a 0.45 μ m nylon membrane before analysis to minimize the adsorbent's interference. After that, the filtered solutions were analyzed for MB uptake analysis by UV-visible spectrophotometer at 664 nm, which is the maximum absorption peak of MB. The adsorption capacity of MB in the aqueous solution was calculated by using Eq. (1) as follows:

$$q_e = [(C_o - C_e)V] / M \quad (1)$$

where C_e (mg/L) and C_o (mg/L) respectively represent the equilibrium and initial concentration of adsorbate, adsorbent mass is denoted by M (g), and solution volume is V (L). The isotherm parameters of the

Langmuir and Freundlich, Temkin and Dubinin-Radushkevich models were investigated using batch experimental adsorption data at various C_o studied. For the kinetic studies, the experiments were carried out similarly as described above. Approximately 2 mL of MB solution was withdrawn at specific time intervals using a plastic syringe. The MB concentration in the liquid phase (C_t , mg/g) was analysed as a function of contact time (t). The adsorption capacity (q_e) was calculated using Eq. (2):

$$q_t = [(C_o - C_t)V] / M \quad (2)$$

where q_t is the amount of MB adsorbed per unit weight of adsorbent at any time t (mg/g); C_o and C_t are the initial and liquid-phase concentrations of the adsorbate solution at any time t (mg/L), respectively; V is the volume of the solution (L); and M is the weight of the sorbent used (g).

The thermodynamic studies were performed similarly as adsorption equilibrium study. The adsorption temperatures were varied from 25, 30, 35 and 40 °C (± 2 °C). These experiments were carried out in incubator shaker at shaking rate of 125 rpm. The BTAC dosage and MB concentration was fixed at 0.05 g and 125 mg/L, respectively. The adsorption capacity of MB in the aqueous solutions was calculated by using Eq. (1). All isotherm, kinetic and thermodynamic studies were fitted with the experimental data using their linear equations which were shown in Table 2.

Table 2. The equations of isotherm, kinetic and thermodynamic studies

Parameters	Equation	Nomenclature
Langmuir	$\begin{aligned} C_e/q_e &= 1/K_L q_m + C_e/q_m ; \\ R_L &= 1/(1 + K_L C_o) \end{aligned} \quad (3)$	q_e = amount adsorbate equilibrium (mg/g) q_t = amount adsorbate retained at time (mg/g) q_m = monolayer adsorption capacity (mg/g) t = time (min)
Freundlich	$\ln(q_e) = \ln(K_F) + 1/n \ln(C_e) \quad (4)$	k_1 = PFO rate constant (1/min) k_2 = PSO rate constant (g/mg.min) k_{ID} = IPD rate constant (mg/g/min ^{0.5}) C_i = thickness of the boundary layer (mg/g)
Temkin	$\begin{aligned} q_e &= B \ln(K_T) + B \ln(C_e) ; \\ B &= RT/b_T \end{aligned} \quad (5)$	k_1 = PFO rate constant (1/min) k_2 = PSO rate constant (g/mg.min) k_{ID} = IPD rate constant (mg/g/min ^{0.5}) C_i = thickness of the boundary layer (mg/g)
Dubinin-Radushkevich	$\begin{aligned} \ln(q_e) &= \ln(q_s) - \beta \varepsilon^2 ; \\ \varepsilon &= RT \ln[1 + 1/C_e] ; \\ E &= 1/\sqrt{2\beta} \end{aligned} \quad (6)$	
Pseudo first order (PFO)	$\ln(q_e - q_t) = \ln(q_e) - k_1 t \quad (7)$	C_i = thickness of the boundary layer (mg/g) K_L = Langmuir adsorption equilibrium constant (L/mg) C_e = equilibrium concentration (mg/L) C_o = initial concentration (mg/L)
Pseudo second order (PSO)	$t/q_t = (1/k_2 q_e^2) + (1/q_e) t \quad (8)$	R_L = separation factor n = adsorption intensity K_F = Freundlich adsorption capacity constant (L/g) b_T = Temkin isotherm constant (mg/L)
Intraparticle diffusion (IPD)	$q_t = k_{ID} t^{0.5} + C_i \quad (9)$	R = gas constant (8.314 J/mol.K) T = absolute temperature (K) q_s = DR adsorption capacity (mg/g) ε = Polanyi potential β = constant related to adsorption energy (mol ² /kJ ²) E = free energy (kJ/mol)
Thermodynamic	$\begin{aligned} \ln K_D &= -\Delta G^\circ / RT \\ \ln K_D &= (\Delta S^\circ / R) - (\Delta H^\circ / RT) ; \\ \Delta G^\circ &= \Delta H^\circ - T \Delta S^\circ \end{aligned} \quad (10)$	k_D = adsorption equilibrium constant (l/mg) ΔG° = free energy (kJ/mol) ΔH° = change in enthalpy (kJ/mol) ΔS° = change in entropy (J/mol.K)

Results and Discussion

Effect of adsorption parameters on MB removal

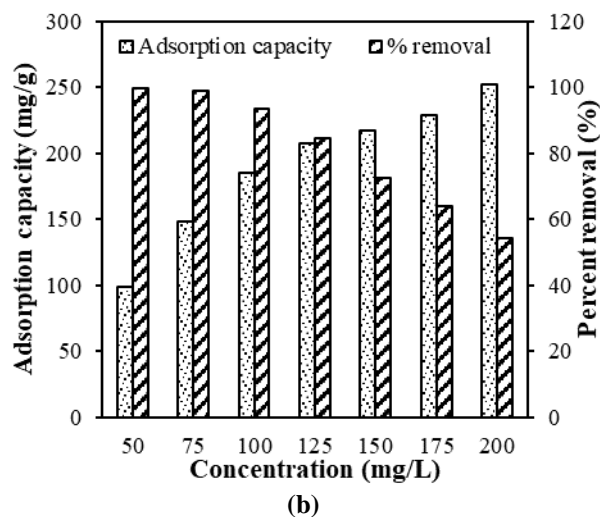
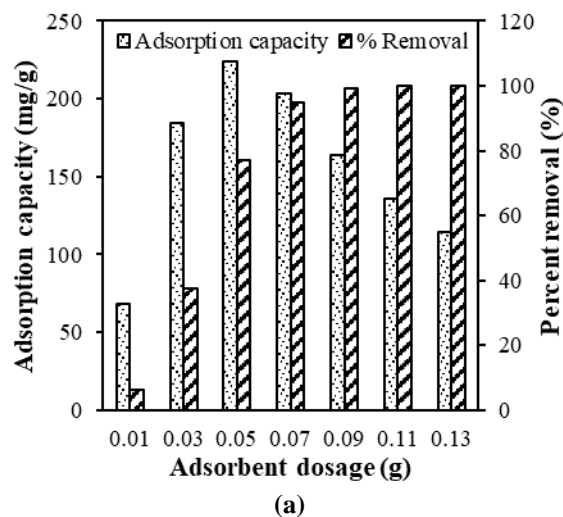
In this study, the preliminary experiments to explore the effect of several adsorption parameters were done by batch adsorption technique. For batch adsorption,

the BTAC is mixed with the MB solution in an agitated vessel for specific time. The effects of adsorbent dosage, initial concentration, contact time and solution pH on adsorption efficiency were presented and described in the following subsections.

Effect of adsorbent dosage

Adsorbent dosage is an important parameter that affects the adsorption performance. This parameter is essential to observe the maximum adsorption with the minimum promising amount of adsorbent [25]. The effect of adsorbent dosage was studied by added different adsorbent dosage (0.01 to 0.13 g) into 100 mL of 150 mg/L MB concentrations under. Figure 1(a) shows the adsorption capacity and percentage removal of MB as a function of the BTAC dose. Adsorption capacity and percent removal of MB increased sharply as the BTAC dose increased from 0.01 to 0.05 g. However, an opposite trend was observed with the additional increased of BTAC dosage beyond 0.05 g. It was noticed that the adsorption capacity of MB start to reduce gradually from 224 to 115 mg/g. Similar trend reduction of adsorption capacity with additional increased in adsorbent dosage were observed by Xue, et al. [19], Muniyandi, et al. [10] and Fan, et al. [26].

While the percentage removal was further increased and reached approximately 100% and did not show any significant MB removal as the BTAC dosage beyond 0.09 g. The opposite relationship between adsorbent dosage and removal of the MB was explained by the existence of a greater number of available sorption sites on adsorbent surface as described by Saif Ur Rehman, et al. [27]. They claimed that the concentration of adsorbate is fixed against an increasing adsorbent dose. Thus, the MB per unit mass of BTAC decreased leaving a number of active sites uncovered at high dosage, subsequently leads to a low adsorption capacity. Hence, considering minimal dosage with the highest adsorption capacity, 0.05 g BTAC dosage was selected as the optimum adsorbent dosage and used for subsequent experiments to study the influence of initial concentration, contact time and solution pH.



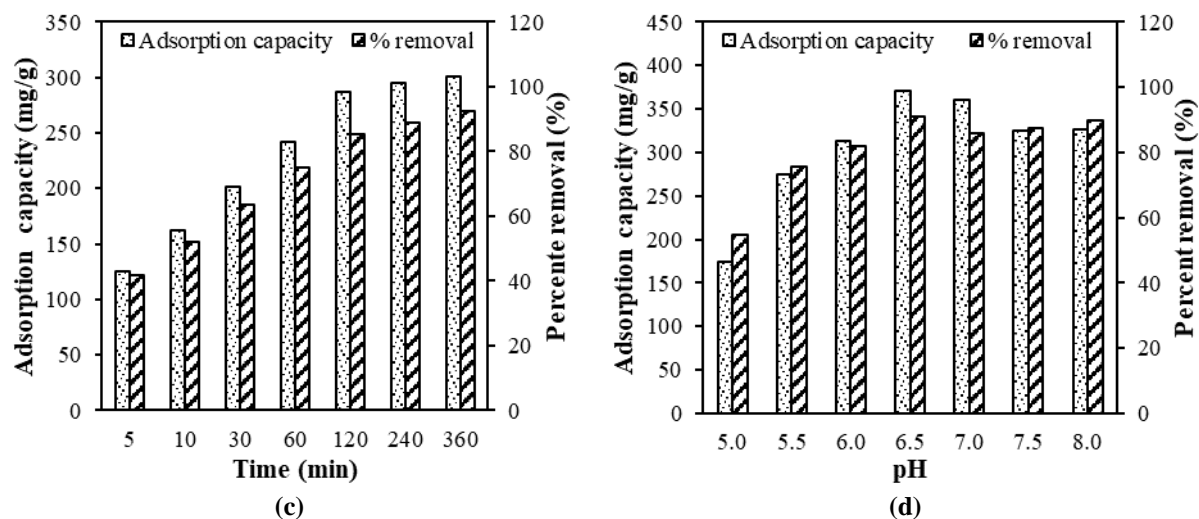


Figure 1. (a) effect of adsorbent dosage (b) effect of initial concentration, (c) effect of contact time and (d) effect of solution pH on the adsorption of MB dye

Effect of initial adsorbate concentration

Initial adsorbate concentration is another important parameter for adsorption study. Figure 1(b) shows an opposite trend of the adsorption capacity and percentage removal of MB as a function of initial MB concentration. Similar observation was reported previously for MB removal by using different type of adsorbent including modified lignocellulosic materials [28]. As per Figure 1(b), the adsorption capacity increased from 98 to 252 mg/g when the initial MB concentration increased from 50 to 200 mg/L. Higher adsorption capacity at high initial concentration is due to the generation of significant driving forces caused by a pressure gradient as explained by Benhouria et al. [29]. However, the percent MB removal gradually decreased from 99 to 54% for a similar increase in MB concentration. This observation related to the at low concentration [30]. This results clearly indicated that the adsorption process is highly dependent on the initial concentration of the solution. Based on the results, MB concentration of 125 mg/L was selected as an optimum concentration as the adsorption capacity was 207 mg/L with the percent removal of 83%, located in the middle of the graph. Thus, this initial concentration was adopted for the next experiment.

Effect of contact time

The influence of contact time (5 to 360 min) on adsorption capacity and MB percent removal is presented in Figure 1(c). Both adsorption capacity and percent removal increased as the function of contact time. When the contact time was approximately 360 min (6 h), the adsorption efficiency reached 92% with 301 mg/g adsorption capacity. It was noticed that the adsorptive removal of MB underwent two stages. During the first stage (within 60 min), the adsorption of MB increased quickly, followed by a slow adsorption stage during which adsorption capacity increased gradually. No further changed observed after 360 min which can be related to adsorption process reached the state of adsorbent–adsorbate equilibrium. This findings suggesting that high attraction existed between MB and the surface of the BTAC and the MB adsorption occurred mainly on the surface at the beginning as described by Li et al. [31]. However, with further extended the contact time, limited surface-active sites were accessible. Therefore, only a minor increase in the adsorption capacity and MB percent removal were observed and this finding mostly due to internal surface adsorption Maneerung et al. [32]. This finding suggested that significant contact time was needed for the adsorbate to diffuse into adsorption sites surface and internal pores of the adsorbent as mentioned by

Jawad et al. [33]. As no further improvement in term of adsorption capacity and MB percent removal were noticed after 360 min, therefore it was determined as an equilibrium contact time between MB and BTAC and was used as a contact time for isotherm study.

Effect of solution pH

The effect of pH on the removal of MB has been investigated. Solution pH was a key factor affecting ionic dyes (anionic or cationic) adsorption because the pH primarily influenced the surface charge on the adsorbent [34]. The adsorption experiment of MB onto BTAC was performed in 5.0 to 8.0 pH range, at controlled temperature of 30 °C for 360 min. Figure 1(d) shows the adsorption capacity and removal efficiency of MB by BTAC under different pH. It was notice that the adsorption capacity was lowest at pH 5.0 (174 mg/g) and the maximum adsorption capacity of the dye was achieved at pH 6.5 (371 mg/g). Similar trend was observed for percentage removal of MB. At the lowest pH (at pH 5.0) the MB removal efficiency was less than 60%. It showed that lower pH does not favour the uptake of cationic dye from the system and leads to electrostatic repulsion. This can be explained as dissolving MB in water results in having positively charged ions in the solution, thereby the positively charged surface of the adsorbent tends toward competing with the adsorption of the MB [35]. However, when the pH increased to 6.5, the MB removal efficiency increased up to 91% due to the decrease in electrostatic repulsion between the positively charged MB and the surface of the BTAC. While with further increase of pH to 7.0, removal efficiency reduced to 85% and no significant changes noticed as the pH increased from 7.0 to 8.0. According to Banerjee and Chattopadhyaya [36], change in pH affects the adsorptive process through the dissociation of functional groups on the adsorbent surface that tends to shift in equilibrium characteristics of the adsorption process. The present findings were supported by earlier reteaches who have reported the removal of MB onto waste carpets derived AC [34] and . Thus, the solution pH of 6.5 was selected as the optimum conditions for adsorption of MB on the surface of the investigated adsorbents.

Isotherm study

In order to study the adsorption behavior of MB in detail, the data for equilibrium adsorption isotherms were fitted into several isotherm models such as Langmuir, Freundlich, Temkin and Dubinin-Raduskevich. The parameters obtained in the isotherm equation and a determination coefficient (R^2) were listed in Table 3. According to the linear regression (R^2) analysis method, it was observed that the values of the correlation coefficients were slightly high (≥ 0.9300). Thus, it showed that the results fit these four models very well. Based on the value of R^2 , the Langmuir isotherm model was the best fit with the adsorption equilibrium data with $R^2=0.9998$. However, according to Misran et al. [2], R^2 is not adequate to depict the applicability of the models to the experimental data. Hence, a comparison was exhibited between the calculated adsorption capacities at equilibrium (q_e) from the applied models and the experimental values. Further analysis of the isotherm data based on root-mean-square error (RMSE) and chi-square (χ^2) analysis showed that the Temkin isotherm model given the lowest values for RMSE and χ^2 analyses. Therefore, Temkin isotherm model was selected as the best fits with the adsorption of MB onto BTAC since it demonstrates better agreement with the experimental data.

Based on the Langmuir isotherm model on the linear Eq. (3), the isotherm parameters, K_L and maximum adsorption capacity, q_m can be determined from the slope of the plot C_e/q_e vs. C_e . In the conditions studied, the maximum adsorption capacity at monolayer coverage (q_m) was 217.4 mg/g. While the calculated R_L values for the selected range of concentration studied were in the range of 0.0045 to 0.0133. These values were greater than zero showing favorable adsorption of MB onto BTAC. Previous study, Ezechi et al. [37] and Fan et al. [26] claimed that for favorable adsorption, $0 < R_L < 1$; unfavorable adsorption, $R_L > 1$; linear adsorption, $R_L = 1$; and adsorption process is irreversible if $R_L = 0$. For the Freundlich isotherm model, the values of n and K_F can be calculated from the plot of $\ln q_e$ vs. $\ln C_e$ using Eq. (4). Based on the equation, the values of n and K_F were 6.9396 and 134.8

L/g, respectively, with $R^2 = 0.9797$. Temkin isotherm represents the quantity of heat needed for the adsorption by one layer of adsorbate on the surface of the adsorbent [38]. Temkin isotherm constants were determined from the slope and intercept from the plot q_e vs. $\ln C_e$ based on the linear Eq. (5). The value of the Temkin constant (B) was calculated to be 22.13 J/mol. The value of B was greater than 1 indicates an exothermic process [39]. While b_T and K_T were calculated to be 111.9 mg/L and 569.2 L/g, respectively. The positive value of b_T proved that the adsorption process was exothermic [35]. Ahmad et al. [40] also observed comparable results for the adsorption study of synthetic dyes removal using pomegranate peel AC. The Dubinin-Radushkevich adsorption isotherm is generally applied to express the adsorption mechanism with a Gaussian energy distribution onto a heterogeneous surface. Based on the Eq. (6), the theoretical saturation adsorption capacity (q_s) and k_{ad} values were calculated to be 172.2 mg/g

and $4 \times 10^{-8} \text{ mol}^2/\text{J}^2$, respectively. While the value of adsorption energy (E) was determined as 3.53 kJ/mol. The value of E was noticed less than 8 kJ/mol implying that removal of MB by BTAC involves physical adsorption as reported by Xue, et al. [19]. Magnitude of E is useful for estimating the mechanism of the adsorption reaction [38]. Based on the result, it can be concluded that strong physical interactions are the driving force of MB adsorption onto BTAC, an assumption supported as well by the great value of saturation adsorption capacity.

The q_m value of MB onto BTAC was then compared with the adsorption capacities of ACs as prepared by various agriculture waste as listed in Table 4. This comparison data clarified that the BTAC is a highly effective adsorbent due to its high surface area and good adsorption capacity for MB dye removal from aqueous solution.

Table 3. Langmuir, Freundlich, Temkin and Dubinin–Radushkevich constants for MB adsorption

Langmuir		Freundlich		Temkin		Dubinin-Radushkevich	
q_m (mg/g)	217.4	n	6.9396	B (J/mol)	22.13	q_s (mg/g)	197.2
K_L (L/mg)	1.4838	K_F (L/g)	134.8	b_T (mg/L)	111.9	k_{ad} (mol^2/J^2)	4.0×10^{-8}
				K_T (L/g)	569.2	E (kJ/mol)	3.53
R^2	0.9998	R^2	0.9797	R^2	0.9671	R^2	0.9304
RMSE	23.22	RMSE	11.60	RMSE	7.72	RMSE	14.48
χ^2	37.72	χ^2	4.58	χ^2	2.27	χ^2	5.74

Table 4. Comparison of MB adsorption capacities by different activated carbon materials

Raw Materials	Surface Area (m^2/g)	MB q_m (mg/g)	References
Banana trunk	1329.5	217.0	This study
Ashitaba biomass	1505.4	323.5	[19]
Sugarcane bagasse	709.3	136.5	[33]
Mangosteen peel	1832.0	871.5	[41]
<i>Myristica fragrans</i> shell	1462.0	346.8	[22]
Fox nutshell shell	2869	249.8	[42]

Kinetic study

In this study, pseudo-first order (PFO) and pseudo-second order (PSO) were used to examine the experimental adsorption data, such as the examination of the controlling mechanisms of the adsorption process (chemical reaction, diffusion control, and mass transfer). The parameter data of the PFO and PSO can be determined from the slope and intercept of plot $\ln(q_e - q_t)$ against t and plot t/q_t against t by the linear Eq. (7) and (8), respectively. The parameters obtained in the PFO and PSO equations, together with their R^2 and $q_{e,cal}$ is listed in Table 3. It was found that the plots $\ln(q_e - q_t)$ against t (Figure 2(a)) give a less linear relationship and subsequently contribute to the low R^2 values. In addition, the experimental and calculated values of q_e showed a significant difference. These results indicate that the experimental data do not agree with PFO kinetic model.

On the other hand, plot t/q_t against t (Figure 2(b)) showed a linear relationship. The R^2 value (~ 0.999) for the PSO kinetic model was relatively higher than the PFO. Moreover, the $q_{e,cal}$ values derived from the PSO model were slightly close to the $q_{e,exp}$ value. Thus, these results suggest that the PSO model provided a good correlation for the adsorption of MB onto BTAC. Most previous studies also report PSO kinetics for adsorption, such as the adsorption of MB onto forest wastes [15], methyl orange onto pumpkin seed powder [43], and adsorption of reactive orange by iron oxide nanospheres [44]. The PSO kinetic model also verified that the chemisorption was the rate-controlling step over the whole adsorption process [45].

The IPD model was also tested because the PFO and PSO kinetic models cannot identify a diffusion

mechanism [46]. Intraparticle models parameters (k_{ID} and C) were calculated from the slope and intercept of plot q_t vs. $t^{1/2}$ and summarized in Table 5. As shown in Figure 2(c), plots of q_t vs. $t^{1/2}$ present multi-linearity, thus indicating that more than one step occurs during the adsorption of MB onto BTAC. Similar patterns have also been obtained by Kumar and Jena [42] and Bedin et al. [47]. According to Shin and Kim [46], the first portion is the fast adsorption or external surface adsorption stage, where adsorbate (MB molecules) migrates through the solution to the exterior surface of the adsorbent (BTAC) particles (Stage I). This portion was attributed to bulk diffusion. The second portion is the gradual adsorption stage, where MB molecules move within the particles (Stage II). This portion is due to intraparticle diffusion. The third portion is the final equilibrium stage, where the MB molecules are adsorbed at sites on the interior surface of BTAC (Stage III). Moreover, the observed multi-linearity also suggests that intraparticle diffusion is not the rate-limiting step [48]. It was observed from Table 5, the value of k_{ID1} and k_{ID2} increase with increasing MB concentration from 75 to 125 mg/L. In addition, at constant MB concentration, the values of k_{ID1} were found larger than k_{ID2} . In other words, the adsorption was rapidly at the initial stage and became slower beyond this stage and no more adsorption occurred when achieving the equilibrium. The magnitude in the C_1 pattern with the changes of adsorbate concentrations was not clearly observed. However, at the second stage, C_2 values were noticed to decrease as the adsorbate concentration increase. The reason behind this due that higher adsorbent dosage will weaker the boundary layer effect.

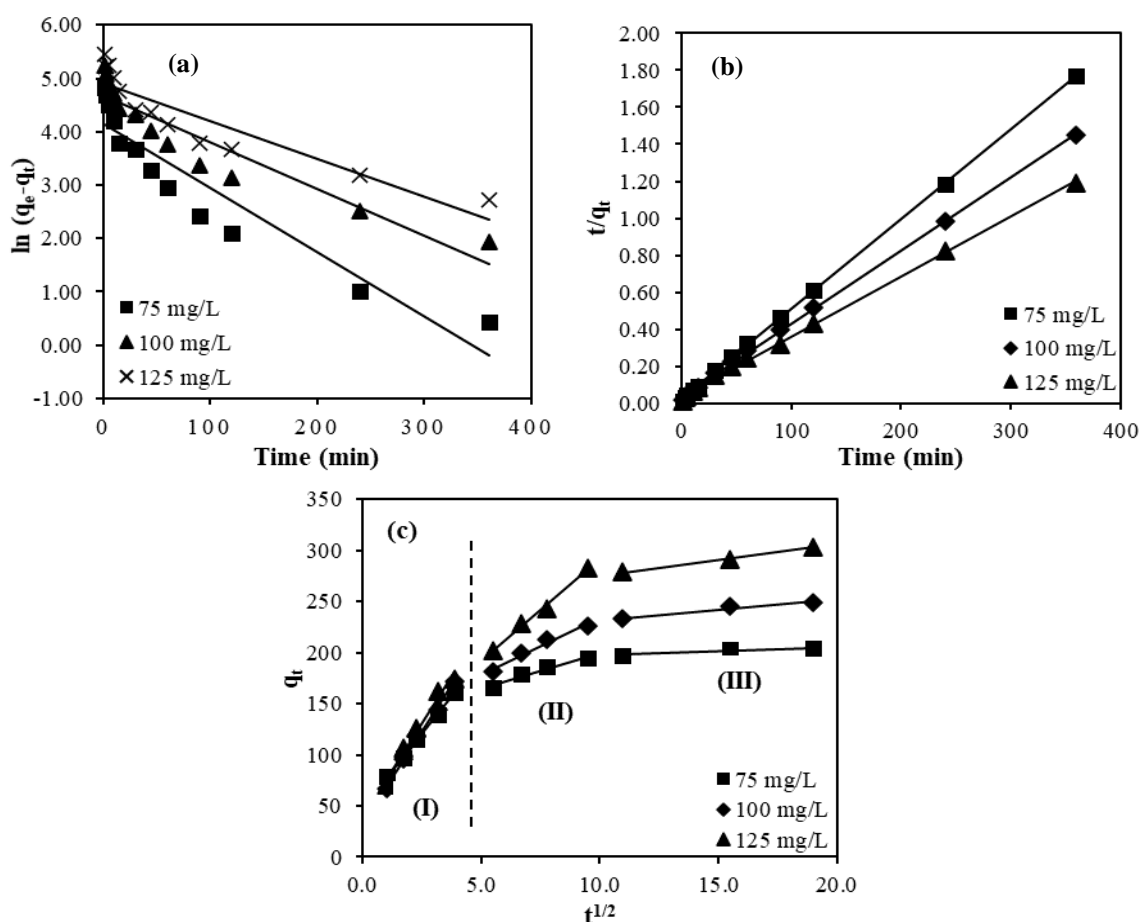


Figure 2. (a) PFO, (b) FSO and (c) IPD model for the adsorption of MB onto BTAC

Table 5. PFO, FSO and IPD parameters for adsorption of MB onto BTAC

Concentration (mg/L)	q _{e,exp} (mg/g)	Kinetic Model					
		Pseudo First Order			Pseudo Second Order		
		q _{e,cal} (mg/g)	k ₁ (1/min)	R ²	q _{e,cal} (mg/g)	k ₂ (g/mg.min)	R ²
75	205.4	62.8	0.0121	0.8841	208.3	0.0010	0.9998
100	255.8	106.5	0.0087	0.8740	250.0	0.0005	0.9992
125	316.2	135.4	0.0071	0.8345	312.5	0.0003	0.9984
Intra-Particle Diffusion Model							
Concentration (mg/L)	k _{ID1} (mg/g.min ^{0.5})	C ₁ (mg/g)	R ²	k _{ID2} (mg/g.min ^{0.5})	C ₂ (mg/g)	R ²	
75	28.722	49.421	0.9978	5.515	139.9	0.9565	
100	35.816	33.619	0.9936	9.192	136.3	0.9710	
125	36.448	40.151	0.9767	19.173	98.0	0.9957	

Thermodynamic study

The slope and the intercept of the plots of $\ln K_D$ versus $1/T$ using the Van't Hoff plot (figure not shown) are used to determine the ΔH° and ΔS° values. From the values of ΔH° and ΔS° , ΔG° can be calculated using Eq. 10. According to the data presented in Table 6, Gibbs free energy (ΔG°) values for MB were in between -25.83 and -26.34 kJ/mol as the temperature rose from 25 to 40 °C. These negative ΔG° values indicate that spontaneous sorption takes place. In addition, the value of ΔG° was observed to increase (less negative) with decreasing temperature, suggesting rapid and more spontaneous adsorption at lower temperatures. In addition, the calculated ΔH° value was -15.57 kJ/mol. The negative value of ΔH° for the adsorption process indicates that the adsorption was an

exothermic process [15]. Furthermore, these results indicate weak attraction forces between the adsorbate and the BTAC. The low value of ΔH° (less than 40 kJ/mol) implies loose bonding between the adsorbate molecules and the adsorbent surface. In the case of entropy (ΔS°), it was found to be 33.87 J/mol.K. The positive value of ΔS° resulted from the increased randomness due to the adsorption of MB, which suggested good affinity of the solute molecules toward the BTAC and increased randomness at the solid-solution interface during the fixation of MB molecules on the active site of the BTAC. A similar finding was also reported by Alver et al. [12] for the adsorption of methylene blue on magnetic alginate/rice husk bio-composite.

Table 6. Thermodynamic study for adsorption of MB

Temperature °C	K_{ad} (L/g)	ΔG° (kJ/mol)	ΔH° (kJ/mol)	ΔS° (J/mol.K)
25	28.48	-25.83	-15.57	33.87
30	25.51	-26.00		
35	23.54	-26.17		
40	21.16	-26.34		

Conclusion

The present investigation revealed that BTAC is a promising adsorbent to remove MB from aqueous solutions. The equilibrium data fitted well to Langmuir, Freundlich, Temkin and Dubinin-Radushkevich isotherm models. Based on error analysis study via RMSE and χ^2 analyses, Temkin isotherm model was the best fitted with the adsorption of MB on BTAC. Maximum monolayer adsorption based on Langmuir was calculated to be 217.4 mg/g. Thermodynamic parameters such as free energy changes (ΔG°), enthalpy (ΔH°) and entropy (ΔS°) were evaluated between temperatures of 25 °C and 40 °C. The ΔG° was noticed progressively decrease from -25.83 to -26.34 kJ/mol as the temperature increase. The ΔH° and ΔS° values were found to be -15.57 kJ/mol and 33.87 J/mol.K respectively. The results showed that the overall adsorption process was exothermic and spontaneous. The findings from this study suggested

that BTAC could be a viable adsorbent in managing higher dye problems associated with textiles industries effluent.

Acknowledgement

This work was supported by Universiti Teknologi MARA (UiTM). Great appreciation goes to the Ministry of Higher Education (MOHE) and members of ASTeRN research interest group for providing support throughout the completion of this research.

References

1. Amran, F. and Zaini, M. A. A. (2021). Sodium hydroxide-activated Casuarina empty fruit: Isotherm, kinetics and thermodynamics of methylene blue and congo red adsorption. *Environmental Technology & Innovation*, 23: 101727.

2. Misran, E., Bani, O., Situmeang, E. M. and Purba, A. S. (2022). Banana stem based activated carbon as a low-cost adsorbent for methylene blue removal: Isotherm, kinetics, and reusability. *Alexandria Engineering Journal*, 61(3): 1946-1955.
3. Wu, J. and Upreti, S. R. (2015). Continuous ozonation of methylene blue in water. *Journal of Water Process Engineering*, 8: 142-150.
4. Hoang, N. T. T., Tran, A. T. K., Hoang, M. H., Nguyen, T. T. H. and Bui, X. T. (2021). Synergistic effect of TiO₂/chitosan/glycerol photocatalyst on color and COD removal from a dyeing and textile secondary effluent. *Environmental Technology & Innovation*, 21: 101255.
5. Singh, J. and Dhaliwal, A. S. (2022). Electrochemical and photocatalytic degradation of methylene blue by using rGO/AgNWs nanocomposite synthesized by electroplating on stainless steel. *Journal of Physics and Chemistry of Solids*, 160: 110358.
6. Sahinkaya, E., Sahin, A., Yurtsever, A. and Kitis, M. (2018). Concentrate minimization and water recovery enhancement using pellet precipitator in a reverse osmosis process treating textile wastewater. *Journal of Environmental Management*, 222: 420-427.
7. Dotto, J., Fagundes-Klen, M. R., Veit, M. T., Palacio, S. M. and Bergamasco, R. (2019). Performance of different coagulants in the coagulation/flocculation process of textile wastewater. *Journal of Cleaner Production*, 208: 656-665.
8. Gnanasekaran, G., Sudhakaran, M. S. P., Kulmatova, D., Han, J., Arthanareeswaran, G., Jwa, E. and Mok, Y. S. (2021). Efficient removal of anionic, cationic textile dyes and salt mixture using a novel CS/MIL-100 (Fe) based nanofiltration membrane. *Chemosphere*, 284: 131244.
9. Sinha, A. K., Sasmal, A. K., Pal, A., Pal, D. and Pal, T. (2021). Ammonium phosphomolybdate [(NH₄)₃PMo₁₂O₄₀] an inorganic ion exchanger for environmental application for purification of dye contaminant wastewater. *Journal of Photochemistry and Photobiology A: Chemistry*, 418: 113427.
10. Muniyandi, M. and Govindaraj, P. (2021). Potential removal of Methylene Blue dye from synthetic textile effluent using activated carbon derived from Palmyra (Palm) shell. *Materials Today: Proceedings*, 47: 299-311.
11. De Gisi, S., Lofrano, G., Grassi, M. and Notarnicola, M. (2016). Characteristics and adsorption capacities of low-cost sorbents for wastewater treatment: a review. *Sustainable Materials and Technologies*, 9: 10-40.
12. Alver, E., Metin, A. Ü. and Brouers, F. (2020). Methylene blue adsorption on magnetic alginate/rice husk bio-composite. *International Journal of Biological Macromolecules*, 154: 104-113.
13. Rohaizad, A., Shahabuddin, S., Shahid, M. M., Rashid, N. M., Hir, Z. A. M., Ramly, M. M., ... and Aspanut, Z. (2020). Green synthesis of silver nanoparticles from *Catharanthus roseus* dried bark extract deposited on graphene oxide for effective adsorption of methylene blue dye. *Journal of Environmental Chemical Engineering*, 8(4): 103955.
14. Arabpour, A., Dan, S. and Hashemipour, H. (2021). Preparation and optimization of novel graphene oxide and adsorption isotherm study of methylene blue. *Arabian Journal of Chemistry*, 14(3): 103003.
15. Gemici, B. T., Ozel, H. U. and Ozel, H. B. (2021). Removal of methylene blue onto forest wastes: Adsorption isotherms, kinetics and thermodynamic analysis. *Environmental Technology & Innovation*, 22: 101501.
16. Li, W., Xie, Z., Xue, S., Ye, H., Liu, M., Shi, W. and Liu, Y. (2021). Studies on the adsorption of dyes, Methylene blue, Safranin T, and Malachite green onto Polystyrene foam. *Separation and Purification Technology*, 276: 119435.
17. Meili, L., Lins, P. V. S., Costa, M. T., Almeida, R. L., Abud, A. K. S., Soletti, J. I., ... and Erto, A. (2019). Adsorption of methylene blue on agroindustrial wastes: experimental investigation and phenomenological modelling. *Progress in Biophysics and Molecular Biology*, 141: 60-71.

18. Shamsabadi, A. S., Bazarganipour, M. and Tavanai, H. (2021). An investigation on the pore characteristics of dates stone based microwave activated carbon nanostructures. *Diamond and Related Materials*, 120: 108662.
19. Xue, H., Wang, X., Xu, Q., Dhaouadi, F., Sellaoui, L., Seliem, M. K., ... and Li, Q. (2022). Adsorption of methylene blue from aqueous solution on activated carbons and composite prepared from an agricultural waste biomass: A comparative study by experimental and advanced modeling analysis. *Chemical Engineering Journal*, 430: 132801.
20. Khairiah, K., Frida, E., Sebayang, K., Sinuhaji, P. and Humaidi, S. (2021). Data on characterization, model, and adsorption rate of banana peel activated carbon (*Musa Acuminata*) for adsorbents of various heavy metals (Mn, Pb, Zn, Fe). *Data in Brief*, 39: 107611.
21. Salem, S., Teimouri, Z. and Salem, A. (2020). Fabrication of magnetic activated carbon by carbothermal functionalization of agriculture waste via microwave-assisted technique for cationic dye adsorption. *Advanced Powder Technology*, 31(10): 4301-4309.
22. Mariana, M., Mistar, E. M., Alfatah, T. and Supardan, M. D. (2021). High-porous activated carbon derived from *Myristica fragrans* shell using one-step KOH activation for methylene blue adsorption. *Bioresource Technology Reports*, 16: 100845.
23. Lewoyehu, M. (2021). Comprehensive review on synthesis and application of activated carbon from agricultural residues for the remediation of venomous pollutants in wastewater. *Journal of Analytical and Applied Pyrolysis*, 159: 105279.
24. Ab Ghani, Z., Yusoff, M. S., Zaman, N. Q., Zamri, M. F. M. A. and Andas, J. (2017). Optimization of preparation conditions for activated carbon from banana pseudo-stem using response surface methodology on removal of color and COD from landfill leachate. *Waste Management*, 62: 177-187.
25. Olu-Owolabi, B. I., Diagboya, P. N. and Ebaddan, W. C. (2012). Mechanism of Pb^{2+} removal from aqueous solution using a nonliving moss biomass. *Chemical Engineering Journal*, 195: 270-275.
26. Fan, S., Wang, Y., Wang, Z., Tang, J., Tang, J. and Li, X. (2017). Removal of methylene blue from aqueous solution by sewage sludge-derived biochar: Adsorption kinetics, equilibrium, thermodynamics and mechanism. *Journal of Environmental Chemical Engineering*, 5(1): 601-611.
27. Saif Ur Rehman, M., Kim, I., Rashid, N., Adeel Umer, M., Sajid, M. and Han, J. I. (2016). Adsorption of brilliant green dye on biochar prepared from lignocellulosic bioethanol plant waste. *CLEAN–Soil, Air, Water*, 44(1): 55-62.
28. Manna, S., Roy, D., Saha, P., Gopakumar, D. and Thomas, S. (2017). Rapid methylene blue adsorption using modified lignocellulosic materials. *Process Safety and Environmental Protection*, 107, 346-356.
29. Benhouria, A., Islam, M. A., Zaghouane-Boudiaf, H., Boutahala, M. and Hameed, B. H. (2015). Calcium alginate–bentonite–activated carbon composite beads as highly effective adsorbent for methylene blue. *Chemical Engineering Journal*, 270: 621-630.
30. Pathania, D., Sharma, S. and Singh, P. (2017). Removal of methylene blue by adsorption onto activated carbon developed from *Ficus carica* bast. *Arabian Journal of Chemistry*, 10: S1445-S1451.
31. Li, Z., Wang, G., Zhai, K., He, C., Li, Q. and Guo, P. (2018). Methylene blue adsorption from aqueous solution by loofah sponge-based porous carbons. *Colloids and Surfaces A: Physicochemical and Engineering Aspects*, 538: 28-35.
32. Maneerung, T., Liew, J., Dai, Y., Kawi, S., Chong, C. and Wang, C. H. (2016). Activated carbon derived from carbon residue from biomass gasification and its application for dye adsorption: kinetics, isotherms and thermodynamic studies. *Bioresource technology*, 200: 350-359.

33. Jawad, A. H., Abdulhameed, A. S., Bahrudin, N. N., Hum, N. N. M. F., Surip, S. N., Syed-Hassan, S. S. A., .. and Sabar, S. (2021). Microporous activated carbon developed from KOH activated biomass waste: surface mechanistic study of methylene blue dye adsorption. *Water Science and Technology*, 84(8): 1858-1872.
34. Hassan, A. F. and Elhadidy, H. (2017). Production of activated carbons from waste carpets and its application in methylene blue adsorption: Kinetic and thermodynamic studies. *Journal of Environmental Chemical Engineering*, 5(1): 955-963.
35. Miraboutalebi, S. M., Nikouzad, S. K., Peydayesh, M., Allahgholi, N., Vafajoo, L. and McKay, G. (2017). Methylene blue adsorption via maize silk powder: Kinetic, equilibrium, thermodynamic studies and residual error analysis. *Process Safety and Environmental Protection*, 106: 191-202.
36. Banerjee, S. and Chattopadhyaya, M. C. (2017). Adsorption characteristics for the removal of a toxic dye, tartrazine from aqueous solutions by a low cost agricultural by-product. *Arabian Journal of Chemistry*, 10: S1629-S1638.
37. Ezechi, E. H., bin Mohamed Kutty, S. R., Malakahmad, A. and Isa, M. H. (2015). Characterization and optimization of effluent dye removal using a new low cost adsorbent: Equilibrium, kinetics and thermodynamic study. *Process Safety and Environmental Protection*, 98: 16-32.
38. Abbas, M. and Trari, M. (2015). Kinetic, equilibrium and thermodynamic study on the removal of Congo Red from aqueous solutions by adsorption onto apricot stone. *Process Safety and Environmental Protection*, 98: 424-436.
39. Nnadozie, E. C. and Ajibade, P. A. (2020). Adsorption, kinetic and mechanistic studies of Pb (II) and Cr (VI) ions using APTES functionalized magnetic biochar. *Microporous and Mesoporous Materials*, 309: 110573.
40. Ahmad, M. A., Puad, N. A. A. and Bello, O. S. (2014). Kinetic, equilibrium and thermodynamic studies of synthetic dye removal using pomegranate peel activated carbon prepared by microwave-induced KOH activation. *Water Resources and industry*, 6: 18-35.
41. Zhang, Z., Xu, L., Liu, Y., Feng, R., Zou, T., Zhang, Y., ... and Zhou, P. (2021). Efficient removal of methylene blue using the mesoporous activated carbon obtained from mangosteen peel wastes: Kinetic, equilibrium, and thermodynamic studies. *Microporous and Mesoporous Materials*, 315: 110904.
42. Kumar, A. and Jena, H. M. (2016). Removal of methylene blue and phenol onto prepared activated carbon from Fox nutshell by chemical activation in batch and fixed-bed column. *Journal of Cleaner Production*, 137: 1246-1259.
43. Subbaiah, M. V. and Kim, D. S. (2016). Adsorption of methyl orange from aqueous solution by aminated pumpkin seed powder: Kinetics, isotherms, and thermodynamic studies. *Ecotoxicology and Environmental Safety*, 128: 109-117.
44. Khosravi, M. and Azizian, S. (2014). Adsorption of anionic dyes from aqueous solution by iron oxide nanospheres. *Journal of Industrial and Engineering Chemistry*, 20(4): 2561-2567.
45. Zhu, C. S., Wang, L. P. and Chen, W. B. (2009). Removal of Cu (II) from aqueous solution by agricultural by-product: peanut hull. *Journal of Hazardous Materials*, 168(2-3): 739-746.
46. Shin, H. S. and Kim, J. H. (2016). Isotherm, kinetic and thermodynamic characteristics of adsorption of paclitaxel onto Diaion HP-20. *Process Biochemistry*, 51(7): 917-924.
47. Bedin, K. C., Martins, A. C., Cazetta, A. L., Pezoti, O. and Almeida, V. C. (2016). KOH-activated carbon prepared from sucrose spherical carbon: Adsorption equilibrium, kinetic and thermodynamic studies for Methylene Blue removal. *Chemical Engineering Journal*, 286: 476-484.
48. Ghani, Z. A., Yusoff, M. S., Zaman, N. Q., Andas, J. and Aziz, H. A. (2017). Adsorptive removal of dissolved organic matter (DOM) in landfill leachate by iron oxide nanoparticles (FeONPs). *AIP Conference Proceedings*, 1892: 040016.